CD10-Bound Human Mesenchymal Stem/Stromal Cell-Derived Exosomes Possess Immunomodulatory Cargo and Maintain Cartilage Homeostasis under Inflammatory Conditions

Dimitrios Kouroupis * , Lee D. Kaplan , Johnny Huard , Thomas M. Best

Posted Date: 22 May 2023

doi: 10.20944/preprints202305.1465.v1

Keywords: Mesenchymal Stem/Stromal Cells (MSC); Synovium; Infrapatellar fat pad (IFP); CD10 (neprilysin); PRG4 (lubricin); Exosomes; Immunomodulation; Pain; Chondroprotection; Inflammatory Joint Diseases

Article

CD10-Bound Human Mesenchymal Stem/Stromal Cell-Derived Exosomes Possess Immunomodulatory Cargo and Maintain Cartilage Homeostasis under Inflammatory Conditions

Dimitrios Kouroupis [1,2,*], Lee D Kaplan [1], Johnny Huard [3] and Thomas M Best [1]

[1] Department of Orthopaedics, UHealth Sports Medicine Institute, University of Miami Miller School of Medicine, Miami, FL, USA
[2] Diabetes Research Institute & Cell Transplant Center, University of Miami Miller School of Medicine, Miami, FL, USA
[3] Linda and Mitch Hart Center for Regenerative and Personalized Medicine, Steadman Philippon Research Institute, Vail, Colorado, USA.
* Correspondence: Dimitrios Kouroupis, MSc, PhD, Department of Orthopaedics, Division of Sports Medicine, Diabetes Research Institute, Cell Transplant Center, University of Miami, Miller School of Medicine 1450NW 10th Ave, Room 3014, Miami, FL 33136, Tel: +1 (305) 243-2228, E-mail: dxk504@med.miami.edu

Abstract: The onset and progression of human inflammatory joint diseases are strongly controlled by the activation of resident synovium/infrapatellar fat pad (IFP) pro-inflammatory and pain-transmitting signaling. We recently reported that intra-articularly injected IFP-derived Mesenchymal Stem/Stromal Cells (IFP-MSC) acquire a potent immunomodulatory phenotype and actively degrade Substance P (SP) via neutral endopeptidase CD10 (neprilysin). Our hypothesis is that IFP-MSC robust immunomodulatory therapeutic effects are largely exerted via their CD10-bound exosomal secretome (IFP-MSC EXOs) by attenuating synoviocyte pro-inflammatory activation and articular cartilage degradation. Herein, IFP-MSC EXOs were isolated from CD10High- and CD10Low-expressing IFP-MSC cultures and their exosomal miRNA cargo was assessed using multiplex methods. Functionally, we interrogated the effect of CD10High and CD10Low EXOs on stimulated by inflammatory/fibrotic cues synoviocytes monocultures and cocultures with IFP-MSC derived chondropellets. Finally, CD10High EXOs were tested in vivo for their therapeutic capacity in an animal model of acute synovitis/fat pad fibrosis. Our results showed that CD10High and CD10Low EXOs possess distinct miRNA profiles. Reactome analysis of miRNAs highly present in exosomes showed their involvement in the regulation of six gene groups, particularly the immune system. Stimulated synoviocytes exposed to IFP-MSC EXOs demonstrated significantly reduced proliferation and altered inflammation-related molecular profiles compared to control stimulated synoviocytes. Importantly, CD10High EXOs treatment of stimulated chondropellets/synoviocytes cocultures indicated a significant chondroprotective effects. Therapeutically, CD10High EXOs treatment resulted in robust chondroprotective effects by retaining articular cartilage structure/composition and PRG4 (lubricin)-expressing cartilage cells in the animal model of acute synovitis/IFP fibrosis. Our study suggests that CD10High EXOs possess immunomodulatory miRNA attributes with strong chondroprotective/anabolic effects for articular cartilage in vivo. The results could serve as a foundation for EXOs-based therapeutics for the resolution of detrimental aspects of immune-mediated inflammatory joint changes associated with conditions such as osteoarthritis (OA).

Keywords: mesenchymal stem/stromal cells (MSC); synovium; infrapatellar fat pad (IFP); CD10 (neprilysin); PRG4 (lubricin); exosomes; immunomodulation; pain; chondroprotection; inflammatory joint diseases

1. Introduction

In inflammatory joint diseases, including certain phenotypes of osteoarthritis (OA), the synovium and IFP tissues serve as origin of pro-inflammatory and articular cartilage degradative

 doi:10.20944/preprints202305.1465.v1

molecules, as well as a source of the pain-transmitting, immune and inflammation modulator neuropeptide, Substance P (SP)[1–8]. In fact, OA-related knee pain may be driving the association with time-to-mortality[9]. Given the current challenges of identifying disease-modifying treatment strategies for patients with OA[10], novel alternatives such as MSC-based therapeutic approaches have yielded encouraging initial clinical results. Early-stage clinical trials using freshly-isolated or culture-expanded MSC derived mainly from bone marrow and adipose tissues have demonstrated clinical superiority when compared with current alternatives such as hyaluronic acid intra-articular placement[11]. Therefore, to reverse these detrimental pathological cascades, we originally focused on MSC-based immunomodulatory therapies, as their paracrine effects actively modulate immune, inflammatory, and fibrotic events[12–15]. We recently reported that human IFP-MSC after transiently engrafting into joint areas of active synovitis/IFP fibrosis show a potent anti-inflammatory/analgesic phenotype by actively degrading SP *via* neutral endopeptidase CD10[16,17].

Concern regarding the potential side effects and increased immunogenicity with MSC-based therapies has led researchers to pursue cell-free treatments focusing on the MSC secretome, especially their exosomes. Exosomes are nanosized (50–200 nm) extracellular vesicles generated via the endosomal pathway[18], and secreted by numerous cells in response to their surrounding milieu. Thus, their contents (*i.e.,* cargo) and lipid shell may carry information that reflects particular changes in the parental. According to our data, the *in vitro* SP degradation capacity of the IFP-MSC was fully recapitulated by their supernatant alone, while, abrogated with a CD10 inhibitor, suggesting the release of active exosome-bound CD10 from the cells[17]. On this basis, further investigations revealed that IFP-MSC derived exosomes (IFP-MSC EXOs) show distinct miRNA and protein immunomodulatory profiles. Specifically, IFP-MSC EXOs infusion into the knee in an acute synovial/IFP inflammation rat model resulted in robust macrophage polarization towards an anti-inflammatory therapeutic M2 phenotype within the synovium/IFP tissues[19]. Overall, preclinical studies have demonstrated that MSC EXOs have strong immunomod-ulatory properties, particularly through the action of miRNAs, which may be capable of targeting the immune system and modulating angiogenesis[10].

We and others have isolated and characterized exosomes from various MSC sources (i.e. bone marrow, umbilical cord, adipose tissues, endometrium), and our results supports a therapeutic potential through a strong anti-inflammatory, anti-fibrotic and angiogenesis-remodeling capacities[19–21]. Our hypothesis is that CD10 expression levels in IFP-MSC are directly related to the immunomodulatory and chondroprotective effects of their derived EXOs. On this basis, CD10High EXOs show potent molecular immunomodulatory profile which significantly affect synoviocytes functionality in inflammatory conditions *in vitro*. Importantly, chondroprotective effects of CD10High EXOs were not only observed in chondropellets/synoviocytes cocultures under inflammatory conditions *in vitro*, but also in an animal model of acute synovitis/IFP fibrosis by retaining articular cartilage structure/composition. These observations provide a rationale for further testing of a viable MSC EXO-based therapeutic modality for synovitis/IFP fibrosis as well as chronic conditions such as OA where articular cartilage degradation is a critical component of the disease.

2. Materials and Methods

Isolation, Culture and Expansion of IFP-MSC

All experiments using human cells were performed in accordance with relevant guidelines and regulations. Human IFP-MSC were isolated from IFP tissue obtained from de-identified, non-arthritic patients (n=3; two males 46 and 67 years old, and one female 44 years old) undergoing elective knee arthroscopy at the Lennar Foundation Medical Center at the University of Miami. Informed consent was obtained from all participants. All procedures were carried out following approval by the University of Miami IRB not as human research (based on the nature of the samples as discarded tissue). IFP tissue (5-10 cc) was mechanically dissected and washed repeatedly with Dulbecco's Phosphate Buffered Saline (DPBS; Sigma Aldrich, St Louis, MO, USA), followed by enzymatic digestion using 235 U/ml Collagenase I (Worthington Industries, Columbus, OH, USA) diluted in DPBS and 1% bovine serum albumin (Sigma) for 2 hours at 37°C with agitation. Enzymatic digestion was inactivated

 doi:10.20944/preprints202305.1465.v1

with complete media with DMEM low glucose GlutaMAX (ThermoFisher Scientific, Waltham, MA, USA) containing 10% fetal bovine serum (FBS; VWR, Radnor, PA, USA), washed and seeded at a density of $1x10^6$ cells/175 cm^2 flask in two different complete media: human platelet lysate (hPL) and chemically-reinforced (Ch-R) media. Complete hPL medium was prepared by supplementing DMEM low glucose GlutaMAX with 10% hPL solution (PL Bioscience, Aachen, Germany). Complete Ch-R medium was prepared by mixing Mesenchymal Stem Cell Growth Medium 2 with supplement provided according to manufacturer's instructions (PromoCell, Heidelberg, Germany). At 48h post-seeding, non-adherent cells were removed by DPBS rinsing and fresh media were replenished accordingly.

All MSC were cultured at 37°C 5% (v/v) CO2 until 80% confluent as passage 0 (P0), then passaged at a 1:5 ratio until P3, detaching them with TrypLE™ Select Enzyme 1X (Gibco, ThermoFisher Scientific) and assessing cell viability with 0.4% (w/v) Trypan Blue (Invitrogen, ThermoFisher Scientific). Specifically, Ch-R and hPL IFP-MSC cultures yielded CD10High and CD10Low IFP-MSC, respectively.

Immunophenotype

Flow cytometric analysis was performed on P3 IFP-MSC (n=3). Briefly, 2.0×10^5 cells were labelled with CD10 monoclonal antibody (Biolegend, San Diego, CA, USA) and the corresponding isotype controls. All samples included a Ghost Red Viability Dye (Tonbo Biosciences, San Diego, CA, USA). Data (20.000 events collected) were acquired using a Cytoflex S (Beckman Coulter, Brea, CA, USA) and analyzed using Kaluza analysis software (Beckman Coulter).

Quantitative real-time PCR (qPCR)

RNA extraction was performed using the RNeasy Mini Kit (Qiagen, Frederick, MD) according to manufacturer's instructions. Total RNA (1µg) was used for reverse transcription with SuperScript™ VILO™ cDNA synthesis kit (Invitrogen), and 10 ng of the resulting cDNA was analysed by qPCR using QuantiFast SYBR Green qPCR kit (Qiagen) and a StepOne Real-time thermocycler (Applied Biosystems, Foster City, CA). For each target, human transcript primers were selected using PrimerQuest (Integrated DNA Technologies, San Jose, CA) (Supplementary Table S1). All samples were analysed in triplicate. Mean values were normalized to GAPDH, expression levels were calculated using the $2^{-\Delta\Delta}$Ct method and represented as the relative fold change of the primed cohort to the naïve (=1).

A pre-designed 90 gene Taqman-based mesenchymal stem cell qPCR array (Stem Cell Technologies, Supplementary Table S1) was performed (n=2) using 1000 ng cDNA per IFP-MSC sample and processed using StepOne Real-time thermocycler (Applied Biosystems). Data analysis was performed using Stem Cell technologies qPCR online analysis tool (Stem Cell Technologies). Sample and Control Ct Values were expressed as $2^{-\Delta\Delta}$Ct (with 38 cycles cut-off point). The expression levels were represented in bar plots ranked by transcript expression levels on a log-transformed scale of sample compared to control cohorts. Bar plots were color-coded by the functional class of genes (namely Stemness, MSC, MSC-related/Angiogenic, Chondrogenic/Osteogenic, Chondrogenic, Osteogenic, Adipogenic). A t-test (unpaired, two-tailed test with equal variance) is used in all statistical analysis and p-values were corrected for multiple comparisons by the Benjamini-Hochberg procedure. CD10High and CD10Low IFP-MSC groups were compared and presented in bar plots.

Isolation and validation of IFP-MSC derived exosomes

CD10High and CD10Low IFP-MSC derived exosomes (EXOs) were isolated from IFP-MSC conditioned media by a stepwise ultracentrifugation method and CD63-immunomagnetic purification. Briefly, conditioned media from IFP-MSC groups cultured in exosome-depleted Ch-R or exosome-depleted hPL media[22] are filtered through a 0.22µm filter to remove debris and large vesicles, and differentially centrifuged for 2,000x*g* for 10 min, 10,000x*g* for 30 min, and ultracentrifuged for 120,000x*g* for 16hr[23]. Pre-enriched exosome preparations were incubated with the Dynabeads®-

 doi:10.20944/preprints202305.1465.v1

based Exosome-Human CD63 Isolation/Detection Reagent (Invitrogen) and using a magnetic separator, exosome preparations are further purified. Samples from each group were assessed for biophysical and biochemical characterization[19].

The functional assessment of IFP-MSC EXOs was performed in a concentration corresponding to exosomes secreted from 1 x 10^6 IFP-MSC. For IFP-MSC EXOs tracking, exosomes were stained with PKH26 red fluorescent membrane staining kit (Fluorescent Cell Linker Kits, Sigma) according to manufacturer's instructions and co-cultured with target cells in functional assessments.

miRNA profile of IFP-MSC EXOs

miRNA was extracted from CD10High and CD10Low EXOs using Total Exosome RNA and Protein Isolation Kit (Thermo Fisher Scientific) according to manufacturer's instructions. Total exosome miRNA (1µg) was used for first-strand cDNA synthesis with All-in-One miRNA First-Strand cDNA Synthesis Kit (GeneCopoeia, Rockville, MD).

Pre-designed human MSC exosome 166 miRNA qPCR arrays (GeneCopoeia) were performed using 1000 ng cDNA per IFP-MSC sample (n=2), and processed using StepOne Real-time thermocycler (Applied Biosystems, LLC). Data analysis was performed using qPCR result with GeneCopoeia's online Data Analysis System (http://www.genecopoeia.com/product/qpcr/analyse/). Mean values were normalized to small nucleolar RNA, C/D box 48 (SNORD48), expression levels were calculated using the $2^{-\Delta Ct}$ method. Putative miRNA interactomes were generated using a miRNet centric network visual analytics platform (https://www.mirnet.ca/). The miRNA target gene data were collected from well-annotated database miRTarBase v8.0 and miRNA-gene interactome network refining was performed with 2.0 betweenness cut-off. Values (with 34 cycles cut-off point) were represented in a topology miRNA-gene interactome network using force atlas layout and hypergeometric test algorithm. miRDB online database (http://mirdb.org) for prediction of functional miRNA targets has been used to correlate highly expressed target genes in macrophages and synoviocytes with specific miRNAs identified by IFP-MSC EXOs miRNA profiling. MirTarget prediction scores are in the range of 0–100% probability, and candidate transcripts with scores ≥ 50% are presented as predicted miRNA targets in miRDB[24].

Synoviocyte inflammation assay

Passage 1 synoviocytes (SYN) were expanded in synoviocyte medium (ScienCell, Carlsbad, CA). Synoviocyte/exosome (SYN/IFP-MSC EXOs) co-cultures were performed using CD10High and CD10Low EXOs for each sample (n=2). Co-cultures were fed with synoviocyte medium + TIC inflammatory/fibrotic cocktail (15 ng/ml TNFα, 10 ng/ml IFNγ, 10 ng/ml CTGF) for 72h.

CCK-8 cytotoxicity assay (Cell Counting Kit-8, Sigma) was performed in SYN TIC and IFP-MSC EXOs/SYN TIC according to manufacturer's instructions. CD10High and CD10Low EXOs cytotoxicity was determined by measuring optical densities of individual wells at 450nm (SpectraMax M5 spectrophotometer, Molecular Devices, San Jose, CA).

RNA extraction from SYN TIC cultures was performed using the RNeasy Mini Kit (Qiagen, Frederick, MD) according to manufacturer's instructions. Total RNA (1µg) was used for reverse transcription with SuperScript™ VILO™ cDNA synthesis kit (Invitrogen). A pre-designed 88 gene Human Synoviocyte array (GeneQuery™ Human Synoviocyte Cell Biology qPCR Array Kit, ScienCell) was performed using 1000 ng cDNA per culture and processed using StepOne Real-time thermocycler (Applied Biosystems, LLC). Mean values were normalized to *ACTB* housekeeping gene, expression levels were calculated using the 2−ΔCt method with 34 cycles cut-off. Values were represented in dot plots as the relative fold change of the CD10High EXOs/SYN TIC or CD10Low EXOs/SYN TIC to SYN TIC (reference sample, 2−ΔCt= X sample/X reference sample).

The functional enrichment analysis was performed using g:Profiler (version e108_eg55_p17_9f356ae) with g:SCS multiple testing correction method applying significance threshold of 0.05[25]. The colors for different evidence codes and for log scale are described in Supplementary Table S2.

Chondropellets/Synoviocytes co-culture assay

Chondrogenic differentiation (0.25x10^6 IFP-MSC/pellet) was induced for 15 days with serum-free MesenCult-ACF differentiation medium (STEMCELL Technologies Inc, Vancouver, Canada). Chondropellets were harvested and chondropellets/synoviocytes transwell co-cultures were performed with and without CD10High EXOs (n=2). Co-cultures were fed with synoviocyte medium + TIC inflammatory/fibrotic cocktail (15 ng/ml TNFα, 10 ng/ml IFNγ, 10 ng/ml CTGF) for 72h.

On day 3, chondropellets were harvested for histology and molecular profiling. For histological analysis, chondropellets were cryosectioned and 6-µm frozen sections were stained with hematoxylin and eosin (Sigma), and 1% toluidine blue (Sigma) for semi-quantitative assessment of pellet structure and chondrogenic differentiation, respectively. For molecular profile analysis, RNA extraction from chondropellets was performed using the RNeasy Mini Kit (Qiagen, Frederick, MD) according to manufacturer's instructions. Total RNA (1µg) was used for reverse transcription with SuperScript™ VILO™ cDNA synthesis kit (Invitrogen). A pre-designed 88 gene Human Osteoarthritis array (GeneQuery™ Human Osteoarthritis and Cartilage repair qPCR Array Kit, ScienCell) was performed using 1000 ng cDNA per culture and processed using StepOne Real-time thermocycler (Applied Biosystems, LLC). Mean values were normalized to *ACTB* housekeeping gene, expression levels were calculated using the 2−ΔCt method with 34 cycles cut-off. Values were represented in a stacked bar plot as the relative fold change of the chondropellets with CD10High EXOs to the chondropellets without CD10High EXOs treatment (reference sample, 2−ΔCt= X sample/X reference sample).

The functional enrichment analysis was performed using g:Profiler (version e108_eg55_p17_9f356ae) with g:SCS multiple testing correction method applying significance threshold of 0.05[25]. The colors for different evidence codes and for log scale are described in Supplementary Table S2.

Mono-iodoacetate model of acute synovial/IFP inflammation

All animal experiments were performed in accordance with relevant guidelines and regulations. The animal protocol was approved by the Institutional Animal Care and Use Committee (IACUC) of the University of Miami, USA (approval no. 21-030 LF) and conducted in accordance to the ARRIVE guidelines[26]. Twelve (#12) 10-week-old male Sprague Dawley rats (mean weight 250 g) were used. The animals were housed to acclimate for 1 week before the experiment initiation. One rat was housed per cage in a sanitary, ventilated room with controlled temperature, humidity, and under a 12/12 hour slight/dark cycle with food and water provided ad libitum.

Acute synovial/IFP inflammation was generated by intra-articular injection of 1 mg of mono-iodoacetate (MIA) in 50 µl of saline into the right knee. Under isoflurane inhalation anesthesia, rat knees were flexed 90º and MIA was injected into the medial side of the joint with a 27G needle using the patellar ligament and articular line as anatomical references. Four (4) days later, a single intra-articular injection of CD10High EXOs in 50 µl of Euro-Collins solution (MediaTech) was performed, having as control: 1) rat knees receiving MIA but not IFP-EXOs (Only MIA group); and 2) healthy rat knees. Animals were sacrificed at day 4 after IFP-EXOs injection (d8 in total). This short exposure to MIA has been shown to induce inflammatory changes within the synovium and adjacent IFP[27].

Cytochemical staining and Lubricin (PRG4) immunolocalization in situ

Rat knee joints were harvested by cutting the femur and tibia/fibula 1 cm above and below the joint line, muscles were dissected and removed, and joints were fixed with 10% neutral buffered formalin (Sigma-Aldrich) for 14 days at room temperature. Knee joints were decalcified, cut along the sagittal plane in half, embedded in paraffin, and serial 4 µm sections obtained. Toluidine blue staining was performed to evaluate the sulfated glycosaminoglycans content of articular cartilage. Masson's trichrome staining was performed to evaluate the collagen type and content of the articular cartilage. Microscope images of cytochemically stained tissues were acquired using x10 and x20 objectives Leica DMi8 microscope with Leica X software (Leica). Histochemical staining quantitative

 doi:10.20944/preprints202305.1465.v1

analysis was evaluated in 3 rat knees per condition and 4 microscopy fields per knee with Fiji/ImageJ software.

For anti-lubricin (anti-PRG4) immunofluorescence staining, sections were permeabilized with 1x PBS + 0.2% Triton X-100 for 20 minutes at room temperature and incubated with blocking buffer (1x PBS + 0.1% Triton X-100 with 1% bovine serum albumin) for 1 hour at room temperature. In between different treatments sections were washed with 1x PBS. Mouse anti-rat PRG4 monoclonal antibody (Sigma) was prepared in blocking buffer (1:500) and sections were incubated at 4 °C overnight. Sections were washed with 1x PBS + 0.01% Triton X-100 and incubated for 2 hours with secondary antibody Alexa Fluor647 conjugated goat anti-mouse IgG antibody (Thermo Fisher Scientific) at room temperature. Controls were incubated with secondary antibody only. All sections were rinsed with 1x PBS, mounted in prolong gold antifade reagent with DAPI (Invitrogen), and microscope images were acquired using x20 objective Leica DMi8 microscope with Leica X software (Leica).

Statistical analysis

Normal distribution of values was assessed by the Kolmogorov-Smirnov normality test. In the presence of a non-normal distribution of the data, one-way or two-way ANOVA were used for multiple comparisons. All tests were performed with GraphPad Prism v7.03 (GraphPad Software, San Diego, CA). Level of significance was set at $p<0.05$.

3. Results &Discussion

Distinct molecular profiles of IFP-MSC based on CD10 protein expression level

CD10 is a surface neutral endopeptidase expressed in multiple cell types including MSC [28,29], with enzymatic activity neutralizing various signalling substrates including Substance P (SP)[30,31]. Specifically, SP is a neuropeptide associated with nociceptive pathways that is secreted by sensory nerve fibres in the synovium and IFP tissues. Upon its secretion it actively affects local inflammatory/immune and fibrotic responses by modulation of cell proliferation, activation and migration to sites of inflammation, and the expression of recruiting chemokines and adhesion molecules[3,4]. Importantly, for the onset and progression of human inflammatory joint diseases SP-secreting sensory nerve fibres predominate over sympathetic fibers in anterior knee pain[7,8,32], whereas SP secretion is increased in synovial fluid during joint inflammation[3]. On this basis, we have previously reported that IFP-MSC can efficiently degrade substance P and suppress T cell proliferation *in vitro*, whereas upon intra-articular infusion *in vivo* IFP-MSC can dramatically reverse signs of synovitis and IFP fibrosis[33,34]. Specifically, our *in vivo* animal studies revealed a correlation between CD10 expression magnitude in IFP-MSC and the reduction or even absence of SP+ fibers in areas of active inflammation and fibrosis for both the synovium and IFP tissues. Based on the correlation between CD10 positivity and therapeutic outcomes, levels around 70% or more should represents an effective therapeutic outcome [33].

In the present study, IFP-MSC cultured in regulatory-complaint media (Ch-R and hPL) media showed similar fibroblast-like morphology but importantly had different CD10 expression levels (Figure 1A). Ch-R cultured IFP-MSC had 96.5±5.6% expression whereas hPL cultured IFP-MSC had 59.2±15.7% expression. According to the abovementioned 70% threshold for an effective therapeutic outcome *in vivo*, we named Ch-R cultures as CD10High (more therapeutic) and hPL cultures as CD10Low (less therapeutic).

Preprints (www.preprints.org) | NOT PEER-REVIEWED | Posted: 22 May 2023 doi:10.20944/preprints202305.1465.v1

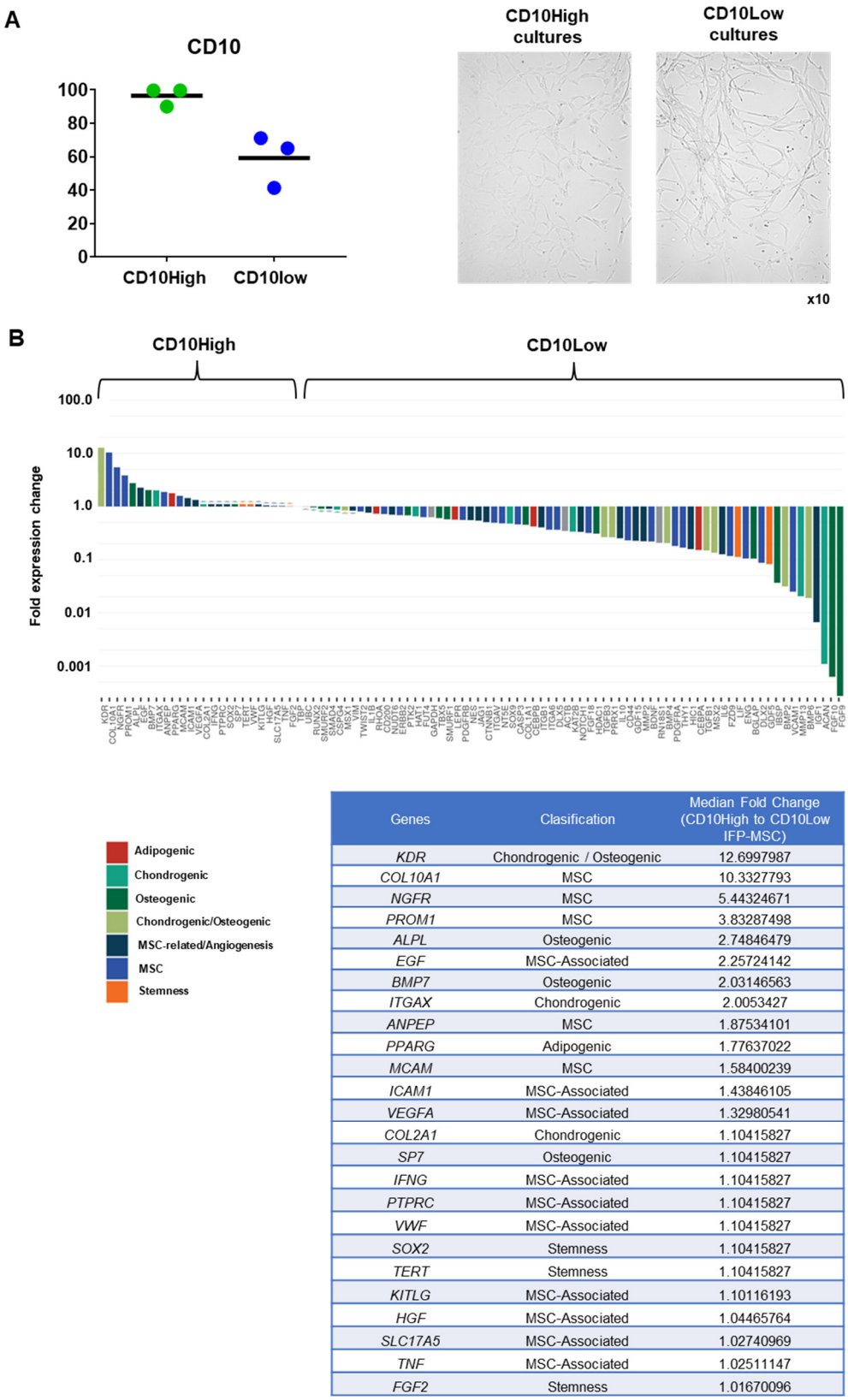

Genes	Clasification	Median Fold Change (CD10High to CD10Low IFP-MSC)
KDR	Chondrogenic / Osteogenic	12.6997987
COL10A1	MSC	10.3327793
NGFR	MSC	5.44324671
PROM1	MSC	3.83287498
ALPL	Osteogenic	2.74846479
EGF	MSC-Associated	2.25724142
BMP7	Osteogenic	2.03146563
ITGAX	Chondrogenic	2.0053427
ANPEP	MSC	1.87534101
PPARG	Adipogenic	1.77637022
MCAM	MSC	1.58400239
ICAM1	MSC-Associated	1.43846105
VEGFA	MSC-Associated	1.32980541
COL2A1	Chondrogenic	1.10415827
SP7	Osteogenic	1.10415827
IFNG	MSC-Associated	1.10415827
PTPRC	MSC-Associated	1.10415827
VWF	MSC-Associated	1.10415827
SOX2	Stemness	1.10415827
TERT	Stemness	1.10415827
KITLG	MSC-Associated	1.10116193
HGF	MSC-Associated	1.04465764
SLC17A5	MSC-Associated	1.02740969
TNF	MSC-Associated	1.02511147
FGF2	Stemness	1.01670096

Figure 1. CD10High and CD10Low IFP-MSC cultures, and their molecular profiling. (A) IFP-MSC cultured in regulatory-complaint media (Ch-R and hPL) media showed similar fibroblast-like morphology but had 96.5±5.6% for Ch-R and 59.2±15.7% for hPL CD10 expression levels. Magnification x10 (B) Molecular profiling of CD10High versus CD10Low IFP-MSC revealed that 25 out of 90 genes tested were higher expressed in CD10High IFP-MSC with 8 genes being more than 2-fold higher (KDR, COL10A1, NGFR, PROM1, ALPL, EGF, BMP7, ITGAX). Interestingly, genes tested were

 doi:10.20944/preprints202305.1465.v1

grouped in phenotype-related cohorts with MSC-associated, Chondrogenic/Osteogenic, and MSC cohorts showing overall the most prominent fold expression change between CD10High and CD10Low IFP-MSC cultures.

Molecular profiling of CD10High versus CD10Low IFP-MSC revealed that 25 out of 90 genes tested were more highly expressed in CD10High IFP-MSC with 8 genes being more than 2-fold higher (*KDR, COL10A1, NGFR, PROM1, ALPL, EGF, BMP7, ITGAX*). Interestingly, genes tested were grouped in phenotype-related cohorts with MSC-associated, Chondrogenic/Osteogenic, and MSC cohorts showing overall the most prominent fold expression change between CD10High and CD10Low IFP-MSC cultures (Figure 1B). Functionally, *KDR (VEGFR2)* and *COL10A1* genes, which are more than 10-fold higher expressed in CD10High IFP-MSC are strongly related to robust pro-chondrogenic and pro-angiogenic MSC actions[35,36]. Interestingly, studies show that the JNK-EGR1 signalling axis promotes TNF-α-induced endothelial differentiation of MSC *via* VEGFR2 expression[35]. COL10A1 is a specific marker of hypertrophic chondrocytes and is critical for endochondral bone formation, as mutation and altered *COL10A1* expression is often accompanied by abnormal chondrocyte hypertrophy in many skeletal diseases[36]. From the highly expressed genes (more than 2-fold), *NGFR (CD271)* and *PROM1 (CD133)* have important roles in pro-angiogenic, immunomodulatory, and chondrogenic MSC actions. In vivo studies showed that $CD271^+$ MSC and $CD133^+$ MSC infusion in ischemia animal models result in increased pro-angiogenic and decrease pro-inflammatory signalling [37,38]. Several studies have associated high NGFR gene and protein expressions in MSC with their increased chondrogenic capacity *in vitro* and osteochondral cartilage repair *in vivo* [39–41]. Pro-chondrogenic and pro-angiogenic actions can be also attributed to MSC with high expression levels of *ALPL, EGF, BMP7,* and *ITGAX* genes[42–44]. Of note, *MCAM (CD146)* gene higher expressed in CD10High IFP-MSC is directly related to increased immunomodulatory MSC actions *in vitro* and *in vivo*[45].

In contrast, CD10Low IFP-MSC molecular profile showed more than 2-fold higher expression of 45 genes compared to CD10High IFP-MSC profile. Specifically, FGF9, FGF10, ACAN, IGF-1 genes seem to be a characteristic molecular signature for CD10Low IFP-MSC as they are expressed more than 150-fold higher, respectively. These genes are involved in proliferation and differentiation MSC signaling. Studies showed that *FGF9* and *FGF10* expression acts as an important regulator of early chondrogenesis partly through the AKT/GSK-3β signaling pathway[46,47]. High *ACAN* gene expression is related to pro-chondrogenic MSC action as its protein is a key GAG-containing proteoglycan in cartilage and plays an important role in stabilizing the ECM in articular cartilage[48]. Also, a recent study showed that IGF-1 transfected MSC have chondroprotective effects in an OA animal model[49].

Overall, CD10 protein levels in MSC strongly affect their molecular profile. CD10High IFP-MSC had a more distinct molecular profile consisting of only 8 genes that were significantly higher expressed (more than 2-fold) compared to CD10Low IFP-MSC. Furthermore, CD10High IFP-MSC molecular profile is related to robust pro-chondrogenic and pro-angiogenic MSC actions.

CD10High and CD10Low EXOs possess immunomodulatory miRNA cargo

Similar to our previous study[19], upon ultracentrifugation and $CD63^+$ immunoselection, both CD10High and CD10Low EXOs show high purity for CD9 (>90%) and <200nm sizes (data not show). From 166 MSC-related miRNAs analyzed, 154 and 151 miRNA cargo were present in CD10High (Figure 2A) and CD10Low eMSC EXOs (Figure 3A), respectively. In CD10High EXOs, 9 miRNAs cargo were predominant (hsa-miR-146a, hsa-miR-4466, hsa-miR-1290, hsa-miR-6089, hsa-miR-1246, hsa-miR-3665, hsa-miR-7975, hsa-miR-4516, hsa-miR-4454) whereas in CD10Low EXOs, 6 miRNAs cargo (hsa-miR-146a, hsa-miR-6089, hsa-miR-4466, hsa-miR-3665, hsa-miR-4454, hsa-miR-7975) were predominant. Furthermore, 2 of the commonly highly present miRNAs (hsa-miR-146a and hsa-miR-6089) are potent regulators of immune system, and specifically T cells and macrophages activation and polarization. The first highly present miRNA cargo, hsa-miR-146a, belongs to the hsa-miR-146 family of genes that are expressed in response to pro-inflammatory stimuli as negative feedback to control inflammation. Specifically, studies showed that hsa-miR-146a negatively regulates the

Preprints (www.preprints.org) | NOT PEER-REVIEWED | Posted: 22 May 2023 doi:10.20944/preprints202305.1465.v1

adaptive immunity by modulating adaptor protein (AP)-1 activity and IL-2 expression in T cells, as well as immune cell activation and cytokine production[50,51]. The second highly present miRNA cargo, hsa-miR-6089 inhibit the activation of macrophages and regulates the generation of IL-6, IL-29, and TNF-α by directly controlling TLR4 signaling[52]. Reactome analysis of miRNAs predominant in CD10High EXOs and CD10Low EXOs showed their involvement in the regulation of six gene groups related to: gene expression, immune system, NGF/PDGF/Wnt pathways, metabolism of proteins, cell cycle, and cellular responses to stress (Figure 2B and Figure 3B).

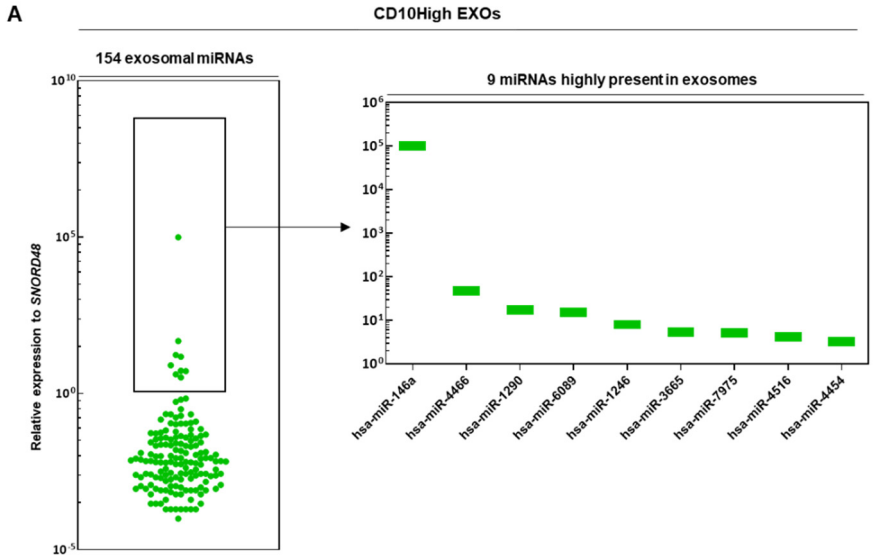

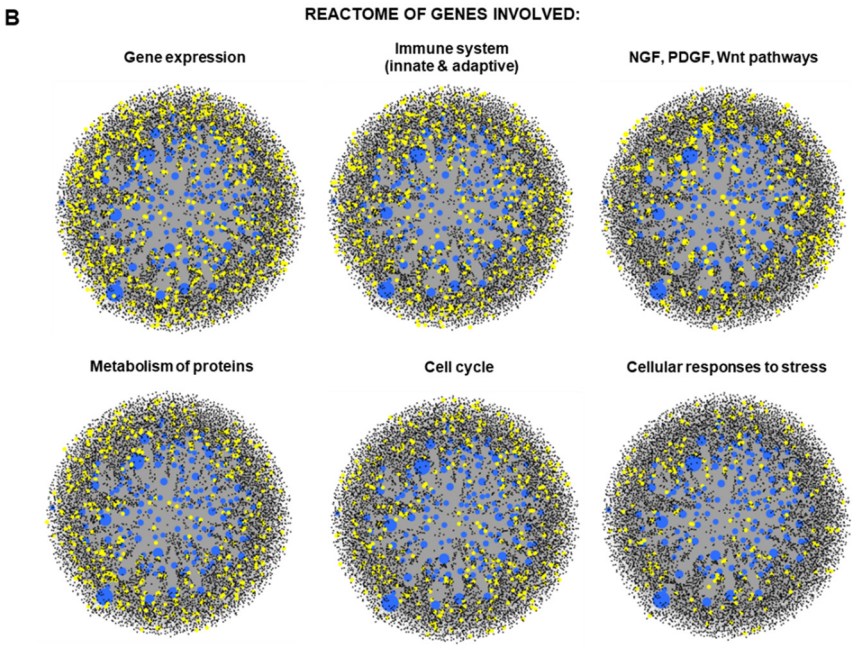

Top Reactome hits	Number of Genes	Pval
Gene Expression	579	2.78E-47
Immune System	513	3.2E-10
Metabolism of proteins	370	3.29E-11
Cell Cycle	328	2.63E-22
Innate Immune System	316	1.14E-07
Adaptive Immune System	246	1.26E-07
Cellular responses to stress	192	3.5E-23
Signalling by NGF	171	2.05E-09
Signaling by Wnt	153	2E-08
Signaling by the B Cell Receptor (BCR)	126	1.85E-09
Signaling by EGFR	118	2.26E-11
Signaling by PDGF	118	3.79E-09

Figure 2. miRNA signature of CD10High EXOs. (A) From 166 MSC-related miRNAs analyzed, 154 miRNA cargo were present in CD10High. In CD10High EXOs, 9 miRNAs cargo are predominant (hsa-miR-146a, hsa-miR-4466, hsa-miR-1290, hsa-miR-6089, hsa-miR-1246, hsa-miR-3665, hsa-miR-

Preprints (www.preprints.org) | NOT PEER-REVIEWED | Posted: 22 May 2023 doi:10.20944/preprints202305.1465.v1

7975, hsa-miR-4516, hsa-miR-4454). (B) Reactome analysis of miRNAs highly present in CD10High EXOs showed their involvement in the regulation of six gene groups related to: gene expression, immune system, NGF/PDGF/Wnt pathways, metabolism of proteins, cell cycle, and cellular responses to stress (blue spots: miRNAs detected in EXOs, black spots: genes related to pathways, yellow spots: genes related to pathway that are affected by miRNAs detected in EXOs).

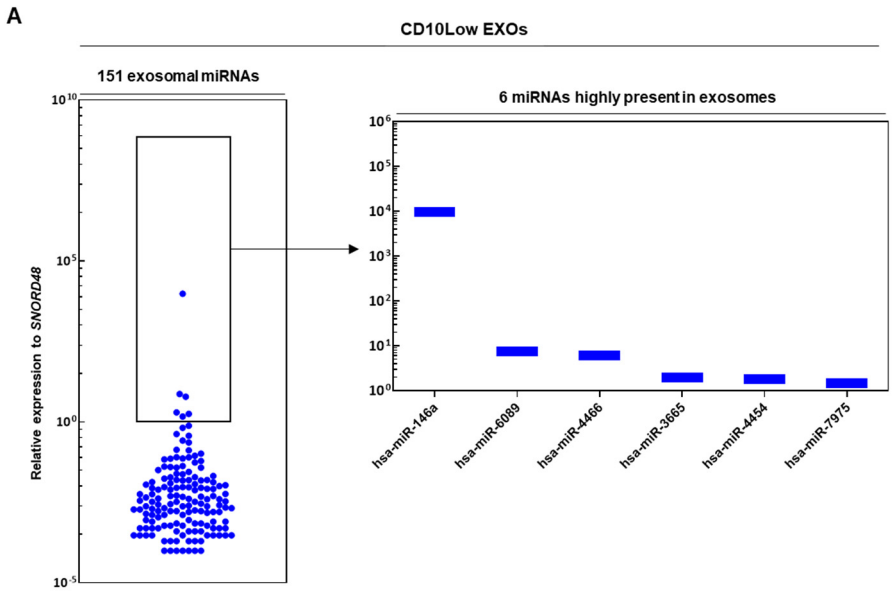

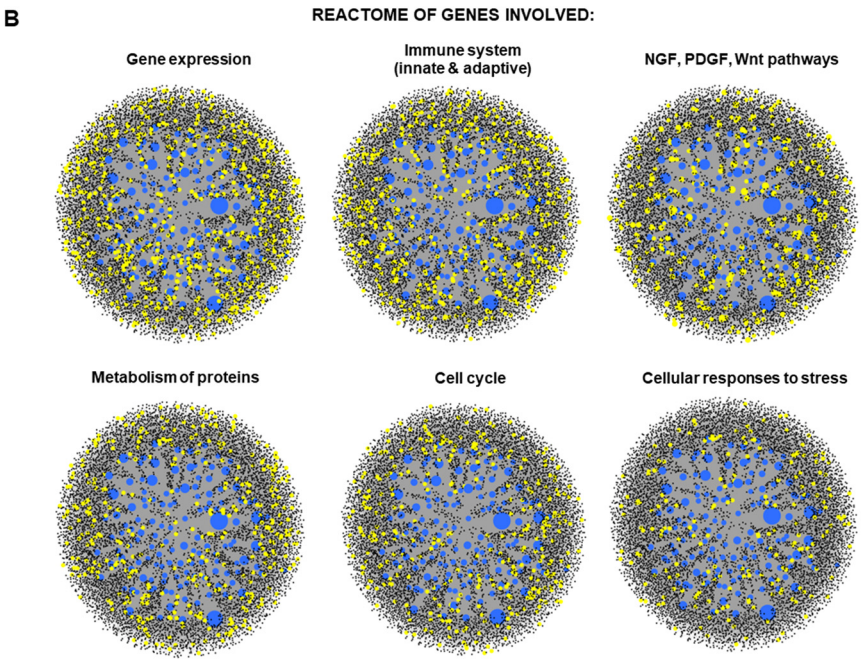

Top Reactome hits	Number of Genes	Pval
Gene Expression	588	1.39E-49
Immune System	514	1.67E-09
Metabolism of proteins	377	3.94E-12
Cell Cycle	328	2.53E-21
Cellular responses to stress	193	4.63E-23
Signalling by NGF	169	2.4E-08
Signaling by Wnt	152	1.01E-07
Generic Transcription Pathway	137	2.76E-14
NGF signalling via TRKA from the plasma membrane	126	2.62E-09
Signaling by the B Cell Receptor (BCR)	123	5.62E-08
Signaling by EGFR	117	1.57E-10
Signaling by PDGF	116	4.91E-08

Figure 3. miRNA signature of CD10Low EXOs. (A) From 166 MSC-related miRNAs analyzed, 151 miRNA cargo were present in CD10Low eMSC EXOs. In CD10Low EXOs, 6 miRNAs cargo are highly present (hsa-miR-146a, hsa-miR-6089, hsa-miR-4466, hsa-miR-3665, hsa-miR-4454, hsa-miR-7975). (B)

 doi:10.20944/preprints202305.1465.v1

Reactome analysis of miRNAs highly present in CD10Low EXOs showed their involvement in the regulation of six gene groups related to: gene expression, immune system, NGF/PDGF/Wnt pathways, metabolism of proteins, cell cycle, and cellular responses to stress (blue spots: miRNAs detected in EXOs, black spots: genes related to pathways, yellow spots: genes related to pathway that are affected by miRNAs detected in EXOs).

Overall, most detected miRNAs were commonly present in IFP-MSC EXOs however 5 miRNAs were specific for CD10High EXOs (hsa-miR-451a, hsa-miR-374a-5p, hsa-miR-525-5p, hsa-miR-499a-5p, hsa-miR-369-3p) and 2 miRNAs were specific for CD10Low EXOs (hsa-miR-132, hsa-miR-218-5p) (Figure 4A). Moreover, the histological profile of the synovium in OA preclinical models[17] and often in OA patients[53] is characterized by synovial lining hyperplasia and IFP fibrosis. The main cellular types contributing to these histological changes are synoviocytes and macrophages polarized towards the pro-inflammatory classical M1 phenotype (reviewed in[54]). On this basis, macrophage phenotype manipulation has been proposed as a potential OA therapy given that initial data, including results from recent studies in our laboratory, indicate polarization of macrophages towards an alternative anti-inflammatory M2 phenotype and IFP fibrosis clearance[16,19].

In the present study, in silico analysis revealed a functional correlation of identified miRNAs in CD10High EXOs and CD10Low EXOs with known highly expressed target genes in macrophages and synoviocytes (Figure 4B). For CD10High EXOs, the prediction scoring system revealed *CCL2* as a target for hsa-miR-374a-5p (92% probability), *CD163* as a target for hsa-miR-369-3p (67% probability), *IL-10* as a target for hsa-miR-374a-5p (68% probability), *TIMP-2* as a target for hsa-miR-369-3p (53% probability), and *PRG4* as a target for hsa-miR-369-3p and hsa-miR-374a-5p (56% and 66%, respectively). Interestingly, hsa-miR-369-3p and hsa-miR-374a-5p CD10High EXOs cargo are potent regulators of anti-inflammatory M2 macrophages phenotype (*CCL2, CD163, IL-10, TIMP-2*)[16,55,56] and lubricin protein production from synoviocytes (*PRG4*)[57]. For CD10Low EXOs, prediction scoring system revealed *TAC1, ARG1, PRG4* as targets for hsa-miR-218-5p (84%, 67%, 80%, respectively). Of note, hsa-miR-218-5p CD10Low EXOs cargo is a potent regulator of inflammation/pain (*TAC1*), anti-inflammatory M2 macrophages phenotype (*ARG1*), and lubricin protein production from synoviocytes (*PRG4*)[16,17,57]. Overall, from a clinical standpoint the potent functionality of these miRNAs strongly support the notion of developing novel cell-free therapeutics for inflammation/fibrosis reversal based on CD10 signature of IFP-MSC EXOs.

Preprints (www.preprints.org) | NOT PEER-REVIEWED | Posted: 22 May 2023 doi:10.20944/preprints202305.1465.v1

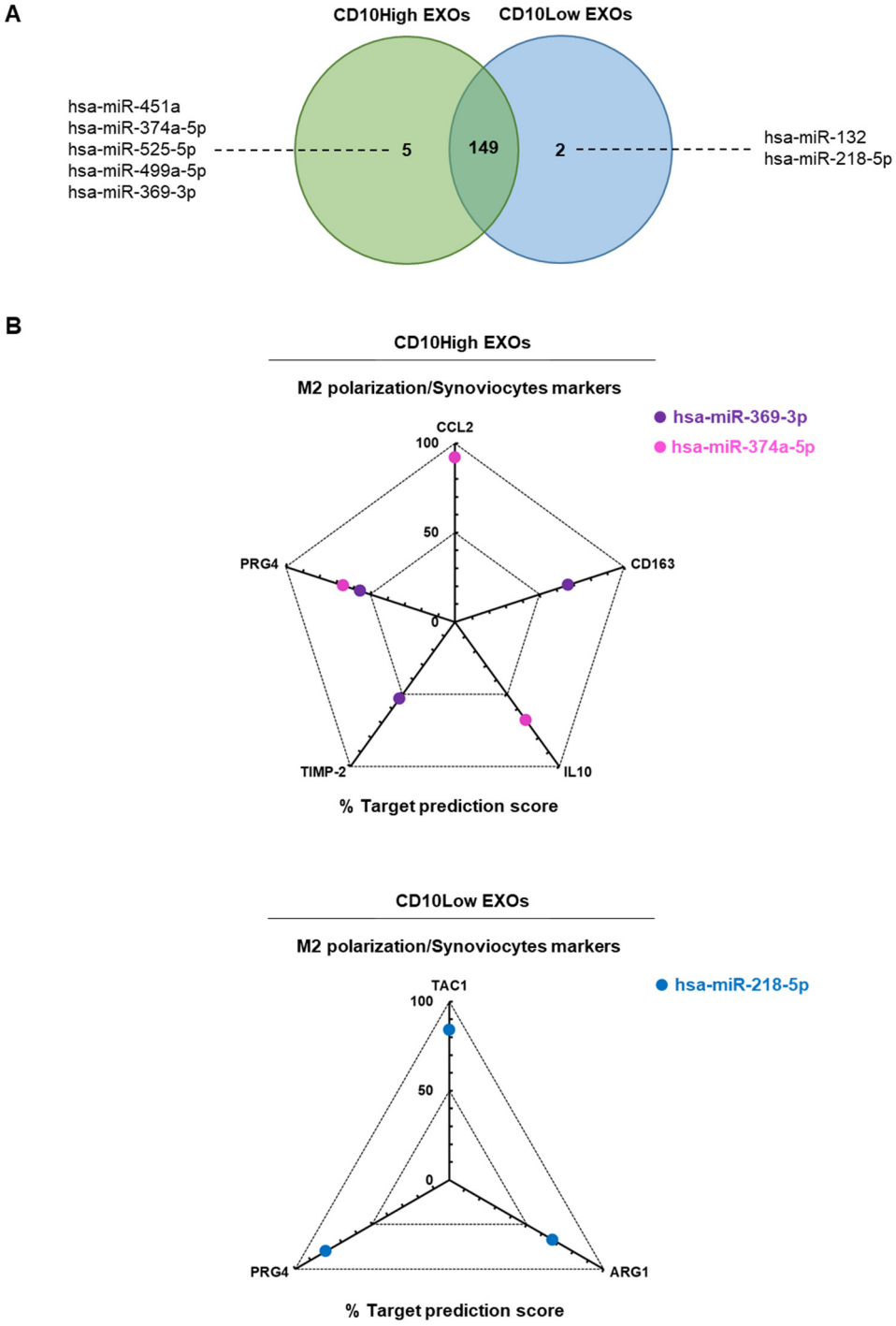

Figure 4. *In silico* analysis for functional correlation of identified miRNAs in IFP-MSC EXOs with known highly expressed target genes in macrophages and synoviocytes. (A) Overall, most detected miRNAs were commonly present in IFP-MSC EXOs however 5 miRNAs were specific for CD10High EXOs (hsa-miR-451a, hsa-miR-374a-5p, hsa-miR-525-5p, hsa-miR-499a-5p, hsa-miR-369-3p) and 2 miRNAs were specific for CD10Low EXOs (hsa-miR-132, hsa-miR-218-5p). (B) For CD10High EXOs, prediction scoring system revealed *CCL2* as a target for hsa-miR-374a-5p (92% probability), *CD163* as target for hsa-miR-369-3p (67% probability), *IL-10* as a target for hsa-miR-374a-5p (68% probability), *TIMP-2* as a target for hsa-miR-369-3p (53% probability), and *PRG4* as a target for hsa-miR-369-3p and hsa-miR-374a-5p (56% and 66%, respectively). For CD10Low EXOs, prediction scoring system revealed *TAC1, ARG1, PRG4* as targets for hsa-miR-218-5p (84%, 67%, 80%, respectively).

Preprints (www.preprints.org) | NOT PEER-REVIEWED | Posted: 22 May 2023 doi:10.20944/preprints202305.1465.v1

CD10High and CD10Low EXOs anti-inflammatory effects on synoviocytes

Synovial lining hyperplasia is a main characteristic of IFP/synovium inflammation in OA. In general, there are two types of resident synoviocytes contributing to this pathological conditions, type A (macrophage-like synoviocytes) and type B (fibroblast-like synoviocytes) are mainly responsible for maintenance of synovial homeostasis[54,58]. Herein, we separately investigated the functional effects of CD10High and CD10Low EXOs on stimulated synoviocytes *in vitro* to identify the optimal therapeutic IFP-MSC EXOs scheme for *in vivo* application.

In co-cultures, both CD10High and CD10Low EXOs were internalized by TIC-primed SYN (SYN TIC) and their proliferation was attenuated (Figures 5A and 5B). This finding suggests that IFP-MSC EXOs, irrespective of the CD10 levels in their parental cells, could attenuate synovial lining hyperplasia upon their *in vivo* intra-articular infusion. Similarly, we and others have reported that SYN exposure to MSC EXOs results in suppressed healthy-SYN[19] and rheumatoid arthritis-SYN[59] activation, migration, and invasion *in vitro*.

At the molecular level, SYN TIC cultures gene expression was strongly affected by both CD10High and CD10Low EXOs. From 88 genes analyzed, most expression levels were down regulated upon exposure to IFP-MSC EXOs (Figure 5C). Specifically, CD10High EXOs increased the expression levels of 45 genes in SYN TIC with only 13 genes being more than two-fold higher (*PTGS2, MDM2, EREG, KRT7, IGF1, ESM1, IL15, ITGA4, VIM, POSTN, CSNK1D, CD14, ALB*). Reactome analysis of highly expressed genes in CD10High EXOs/SYN TIC showed their involvement in the regulation of 5 molecular pathways related to the: regulation of cell population proliferation, cellular response to stimulus, prostaglandin biosynthetic process, regulation of neuroinflammatory response, regulation of protein phosphorylation (Figure 5D). Also, CD10Low EXOs increased the expression levels of 19 genes in SYN TIC with only 9 genes being more than two-fold higher (*PTGS2, EREG, MDM2, KRT7, NGF, POSTN, CD14, ESM1, ITGA4*). Reactome analysis of highly expressed genes in CD10Low EXOs/SYN TIC showed their involvement in the regulation of 5 molecular pathways related to the: regulation of cell population proliferation, regulation of protein phosphorylation, cellular response to stimulus, prostaglandin biosynthetic process, and regulation of cellular senescence (Figure 5D).

From the commonly expressed genes, *PTGS2 (COX2)* is the highest expressed (more than 500-fold) after IFP-MSC EXOs exposure compared to SYN TIC cultures alone. Importantly, *PTGS2* plays crucial role in the promotion of prostaglandin E2 (PGE2) biosynthesis pathway in fibroblast-like cells (such as MSC) indicating its strong involvement in cells' immunomodulatory capacity *in vivo*[60]. On this basis, *via* COX2-dependent PGE2 secretion fibroblast-like cells can polarize macrophages to an alternative anti-inflammatory M2 phenotype, attenuate T cell proliferation and differentiation to Th17, and increase T cells differentiation to Tregs (reviewed in [60]). In parallel, a pioneering study showed an COX2-dependent PGE2 regulated suppression of fibroblasts proliferation[61] that in our data could explain the reduction of synoviocytes proliferation upon exposure to IFP-MSC EXOs. From the highly expressed genes (more than 50-fold), *EREG* and *MDM2* have important pro-survival and trophic roles in synoviocytes. Studies showed that EREG (Epiregulin), a ligand for epidermal growth factor receptor (EGFR), can affect EGFR signaling which is critical for maintaining the superficial layer of articular cartilage and preventing osteoarthritis initiation[62]. Studies showed that *MDM2* higher gene expression in fibroblast-like cells result in higher extracellular matrix accumulation (collagens and fibronectin)[63]. However, MDM2 which is an ubiquitin ligase and binds p53 transcriptional factor for apoptotic pathway, has been associated with rheumatoid arthritis promotion[64]. Although, this is only a part of the pleiotropic IFP-MSC EXOs actions on synoviocytes, these findings invite studies involving OA.

Preprints (www.preprints.org) | NOT PEER-REVIEWED | Posted: 22 May 2023 doi:10.20944/preprints202305.1465.v1

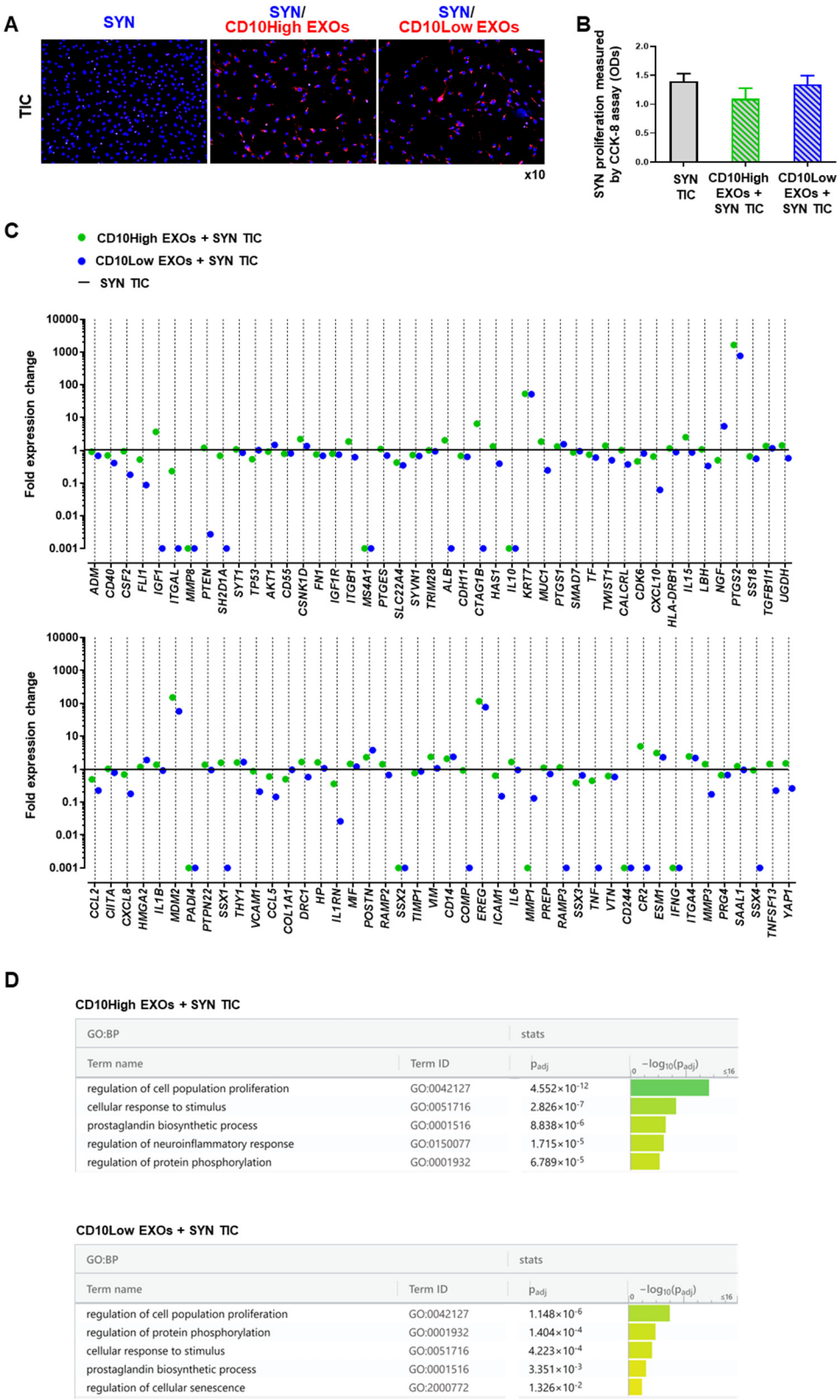

Figure 5. CD10High and CD10Low EXOs anti-inflammatory effects on synoviocytes. (A,B) Both CD10High and CD10Low EXOs were internalized by TIC-primed SYN (blue, nucleus; red, EXOs) whereas they tend to attenuate SYN TIC proliferation. (C) At the molecular level, SYN TIC cultures gene expression was strongly affected by both CD10High and CD10Low EXOs. Specifically, CD10High EXOs increased the expression levels of 45 genes in SYN TIC with only 13 genes being more than two-fold higher. Moreover, CD10Low EXOs increased the expression levels of 19 genes in SYN TIC with only 9 genes being more than two-fold higher. (D) Reactome analysis of highly

 doi:10.20944/preprints202305.1465.v1

expressed genes in CD10High EXOs/SYN TIC and CD10Low EXOs/SYN TIC showed their involvement in the regulation of 5 molecular pathways.

Except the commonly highly expressed genes, CD10High EXOs exposed SYN TIC show additional expression of genes (such as *IGF-1* and *ALB*) involved in synovial fluid enrichment with anabolic factors for cartilage homeostasis. *IGF-1* gene expression is associated with insulin-like growth factor (IGF) signaling pathway activation that can promote chondrocyte proliferation, enhance matrix production, and inhibit chondrocyte apoptosis[65]. Also, high *ALB* gene expression is related to increased production from synoviocytes of albumin, the most common protein in synovial fluid, which plays an important role in the lubrication of the cartilage, thereby protecting the joint cartilage surface from the degradation[66]. Therefore, due to more potent and pleiotropic effects of CD10High EXOs on synoviocytes at the molecular level, we used CD10High EXOs as our platform for further *in vitro* and *in vivo* experimentation.

CD10High EXOs-treated chondrocytes show chondroprotective molecular profile in inflammatory conditions in vitro

At the early onset of inflammatory joint diseases, synovium/IFP anatomical and functional unit[67] serve as a site for immune cell infiltration, neovascularization, origin of pro-inflammatory and articular cartilage (AC) catabolic molecules[11,68]. In this pathological microenvironment, chondrocytes become sensitive to pro-inflammatory mediators, especially tumor necrosis factor-α (TNFα) and interleukin-1β (IL-1β), which initiate the degradation of cartilage extracellular matrix mediated by matrix-metalloproteinases (MMPs), a disintegrin and metalloproteinase with thrombospondin motifs[11]. Herein, we simulated this pro-inflammatory microenvironment *in vitro* by co-culturing MSC-derived chondropellets with inflamed synioviocytes (Figure 6A).

Initially, IFP-MSC were successfully induce towards chondrogenesis in 3-D micromass pellets cultures for 15 days. On this basis, we totally acknowledge that despite MSCs' ability to differentiate toward the chondrogenic lineage, their terminal phenotype is reminiscent of one following endochondral bone formation rather than articular cartilage chondrocytes. However, we and others have demonstrated that on day 15 MSC have adequately differentiated and possess most of major characteristics of chondrocytes without entering hypertrophy and mineralization *in vitro*[33,69,70]. Subsequently, our generated chondropellets and SYN were co-cultured with and without CD10High EXOs under inflammatory/fibrotic TIC conditions for 3 days. Chondropellets histological analysis revealed that although CD10High EXOs-treated and non-treated have similar structure, CD10High EXOs treatment result in better chondrocyte differentiation and sulfated glycosaminoglycans production *in vitro* (Figure 6B).

Preprints (www.preprints.org) | NOT PEER-REVIEWED | Posted: 22 May 2023 doi:10.20944/preprints202305.1465.v1

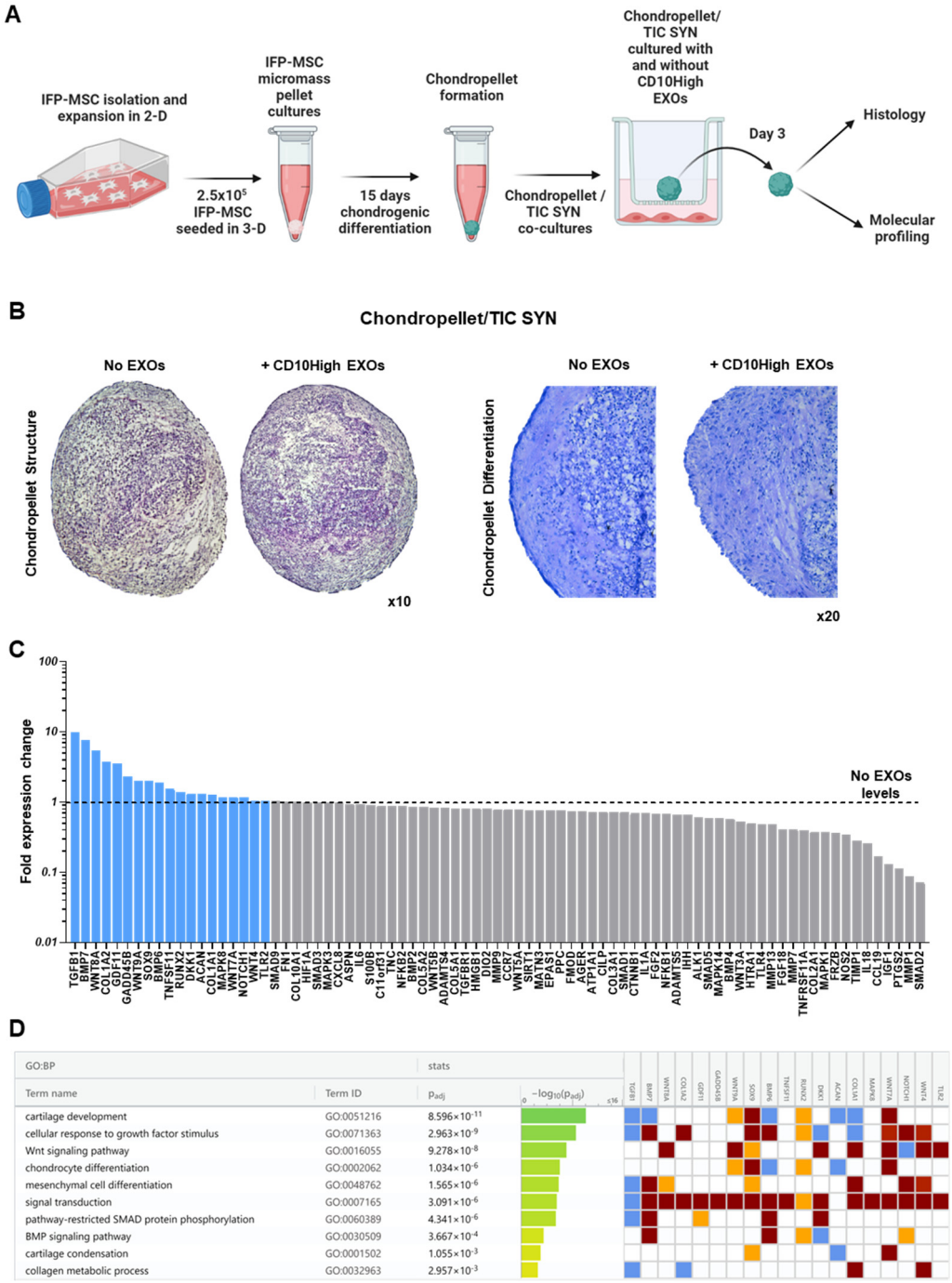

Figure 6. Effects of CD10High EXOs on chondrocytes *in vitro*. (A) Experimental strategy to simulated pro-inflammatory microenvironment *in vitro* by co-culturing MSC-derived chondropellets with inflamed synioviocytes. (B) Chondropellets histological analysis revealed that although CD10High EXOs-treated and non-treated have similar structure, CD10High EXOs treatment result in better chondrocyte differentiation and sulfated glycosaminoglycans production *in vitro*. (C) At the molecular level, CD10High EXOs-treated chondropellets showed distinct transcriptional signature with higher expression of 19 genes. (D) Reactome analysis of highly expressed genes in CD10High EXOs-treated chondropellets showed their involvement in the regulation of 10 chondroprotection- and cartilage homeostasis-related molecular pathways.

At the molecular level, CD10High EXOs-treated chondropellets showed distinct transcriptional signature with higher expression of 19 genes (*TGFB1, BMP7, WNT8A, COL1A2, GDF11, GADD45B, WNT9A, SOX9, BMP6, TNFSF11, RUNX2, DKK1, ACAN, COL1A1, MAPK8, WNT7A, NOTCH1, WNT4, TLR2*) out of 88 genes tested compared to non-treated chondropellets (Figure 6C). Reactome

Preprints (www.preprints.org) | NOT PEER-REVIEWED | Posted: 22 May 2023 doi:10.20944/preprints202305.1465.v1

analysis of highly expressed genes in CD10High EXOs-treated chondropellets showed their involvement in the regulation of 10 chondroprotection- and cartilage homeostasis-related molecular pathways (Figure 6D). Specifically, 7 genes showed more than 2-fold higher expression (*TGFB1, BMP7, WNT8A, COL1A2, GDF11, GADD45B, WNT9A*) in CD10High EXOs-treated chondropellets. Functionally, *TGFB1, BMP7*, and *WNT8A* genes, which are more than 5-fold higher expressed are strongly related to robust cartilage homeostasis effects. Both, TGFB1 and BMP7 are major articular cartilage homeostasis growth factors as they arrest chondrocytes differentiation at an early stage of hypertrophy and inhibit expression of *COL10A1, VEGF, MMP13,* and *BGLAP* (osteocalcin)[43,71]. Interestingly, studies showed that canonical Wnt signaling, *via* Wnt8A gene expression, skews TGFB signaling in chondrocytes towards anabolic signaling *via* ALK1 and Smad 1/5/8[72]. From the more than 2-fold higher expressed genes, *COL1A2* and *GDF11* genes are strongly related to chondrocytes proliferation/differentiation and extracellular matrix synthesis[73,74]. Of note, study showed that in normal articular cartilage approximately 9% of chondrocytes are positive for COL1A2 (collagen type I) protein whereas significant increase in COL1A2 is observed in cartilage degeneration[74]. Finally, *GADD45B* expression enhances *COL10A1* transcription *via* the MTK1/MKK3/6/p38 axis in terminally differentiating chondrocytes[75], whereas *WNT9A* signaling is required for joint integrity and regulation of Indian hedgehog (Ihh) during chondrogenesis[76]. Overall, our data show that CD10High EXOs possess potent chondroprotective and anabolic effects for chondrocytes *in vitro*.

CD10High EXOs show chondroprotective and anabolic effects for articular cartilage in vivo

We have previously reported that functionally IFP-MSC EXOs can significantly reduce synovitis/IFP fibrosis and, also affect macrophage polarization towards an anti-inflammatory therapeutic M2 phenotype in inflammatory conditions *in vivo*[19]. Herein, an acute synovial/IFP inflammation rat (MIA) model was used to test the chondroprotective capacity of CD10High EXOs upon intra-articular infusion to reverse cartilage degeneration *in vivo* (Figure 7A).

Collagen type II and aggrecan are two major components of the extracellular matrix of healthy articular cartilage. Alterations in cartilage extracellular matrix composition and structure are characteristics of OA. Specifically, during OA progression degrading cartilage proteins such as matrix metalloproteinases and aggrecanases result in decreased collagen type II/aggrecan contents, and loss of cartilage integrity[77,78]. In our study, the diseased group (MIA only) demonstrated strong cartilage degeneration signs by reduced staining for sulfated proteoglycans compared to healthy rat knees (Figures 7B and 7C, upper panels). According to the Udo et al. cartilage scoring system (0-5) for rat OA in the MIA model[27], only the diseased group developed grade 3 cartilage erosion (≤50% of joint surface). Importantly, CD10High EXOs intra-articular infusion resulted in significantly ($p<0.05$) reduced cartilage degeneration with only minor cartilage depressions compared to diseased group (average scores 0.4±0.5 and 1.7±1.1, respectively). Masson's Trichrome staining has also been used as a suitable histochemical method[79] to evaluate collagen compositional changes. In general, diseased group showed increased cartilage discoloration (stained as red) compared to other groups. In contrast, CD10High EXOs intra-articular infusion resulted in significantly ($p<0.05$) increased collagen composition similar to the healthy control group (Figures 7B and 7C, middle panels). Similar to our findings, previous studies using intra-articular infusions of MSC EXOs derived from various tissue sources such as bone marrow, amniotic fluid, and umbilical cord, reported the anabolic effects of EXOs to enhance matrix synthesis of collagen type II and sulfated glycosaminoglycans (reviewed in [80]). However, in our study for the first time we demonstrate the chondroprotective effects of CD10High EXOs derived from IFP tissue to articular cartilage.

Preprints (www.preprints.org) | NOT PEER-REVIEWED | Posted: 22 May 2023 doi:10.20944/preprints202305.1465.v1

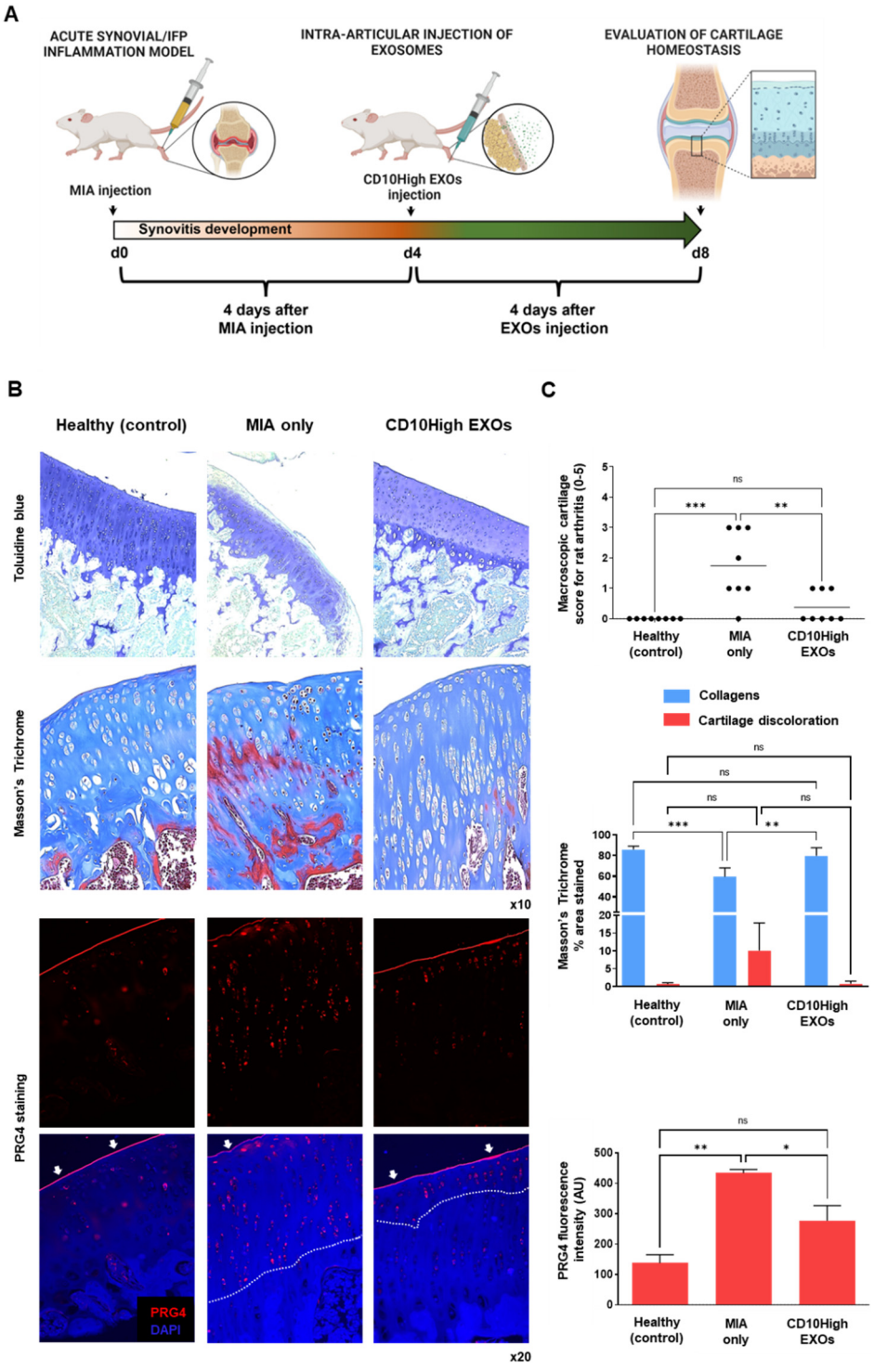

Figure 7. Effects of CD10High EXOs on articular cartilage homeostasis *in vivo*. (A) Schematic indicating the generation of acute synovitis/IFP fibrosis rat model, IFP-MSC EXOs therapeutic intervention and chronological evaluation. (B and C) Toluidine blue staining (top panel), Masson's trichrome staining (middle panel) and PRG4 immunolocalization (lower panels) in sagittal-sectioned knees of representative rats for healthy, diseased (MIA only) or CD10High EXOs treated groups. The diseased group demonstrated strong cartilage degeneration findings exemplified by reduced staining for sulfated proteoglycans. In contrast, CD10High EXOs intra-articular infusion resulted in significantly reduced cartilage degeneration with only minor cartilage depressions and significantly increased collagen composition. Compared to the diseased group, the CD10High EXOs group showed preservation of PRG4 expression on the upper cartilage surface and only minor expression from the intermediate

zone chondrocytes (indicated by white arrows and dotted lines, ns: non-significant, *$p<0.05$, **$p<0.01$, ***$p<0.001$).

The avascular nature of articular cartilage limits the capacity for perivascular MSC to migrate from the neighboring microenvironment (*i.e.* subchondral bone) and restore inflammation/tissue imbalance. However, a pool of resident cartilage-derived stem/progenitor cells (CSPC) is present in the upper zone cartilage zone, associated with the expression of proteoglycan 4 (PRG4) encoding for proteoglycan 4 or lubricin[81,82]. Interestingly, studies showed that CPSC is an intermediate cell population between MSC and differentiated chondrocytes which can be stimulated to induce tissue healing and homeostasis at different stages of cartilage degradation *in vivo*[83,84]. On this basis, we performed *in situ* PRG4 protein expression evaluations to determine phenotypic cellular changes promoted in articular cartilage in disease and after intra-articular CD10High EXOs infusion (Figure 7B and 7C, bottom panels). In our study, the healthy group showed a rigid distinct PRG4+ CSPC upper layer on articular cartilage. In the diseased group, PRG4 expression exhibited a reduction in the upper layer of articular cartilage, and simultaneously a significant ($p<0.05$) increase in the intermediate zone randomly distributed within chondrocytes. This phenomenon can be attributed to the fact that intermediate zone chondrocytes increase the expression of PRG4 in order to replenish the significant loss from the upper cartilage surface during disease progression. Notably, CD10High EXOs intra-articular infusion resulted in significantly ($p<0.05$) preservation of PRG4 expression on the upper cartilage surface and only minor expression from the intermediate zone chondrocytes. This effect can be attributed not only to the general CD10High EXOs immunomodulatory/chondroprotective miRNA profile (Figure 2), but also more specifically to the presence of hsa-miR-369-3p and hsa-miR-374a-5p miRNAs cargo that strongly affect *PRG4* gene expression in target cells (Figure 4B). Therefore, CD10High EXOs treatment suggest robust chondroprotective and anabolic effects from articular cartilage *in vivo*.

Conclusions:

In summary, CD10High EXOs show potent molecular immunomodulatory and chondroprotective profiles that significantly affect synoviocytes and chondropellets functionality in inflammatory conditions *in vitro*. Notably, in an animal model of acute synovitis/IFP fibrosis, CD10High EXOs intra-articular infusion resulted in robust chondroprotective and anabolic effects that retain articular cartilage structure/composition. However, this study has some limitations that deserve consideration. Specifically, the effects of CD10High EXOs in post-traumatic OA (PTOA) animal models with more advanced OA (structural/compositional alterations of articular cartilage) should be investigated in further experiments. Therefore, based on our findings, we propose a proof-of-concept viable cell-free CD10-based EXOs alternative to MSC-based therapeutics in the treatment of inflammatory joint diseases and even OA characterized by synovitis/IFP fibrosis and articular cartilage degradation. Further investigations are needed to strongly support the robust CD10High EXO therapeutic effects in various joint OA phenotypes.

Author Contributions: Conceptualization, DK; methodology, DK; software, DK; validation, DK; formal analysis, DK; investigation, DK; resources, DK, TB, and LK; data curation, DK; writing—original draft preparation, DK; writing—review and editing, DK, TB, JH and LK; visualization, DK; supervision, DK; project administration, DK; funding acquisition, DK, TB, and LK. All authors have read and agreed to the published version of the manuscript.

Funding: This research was funded by National Institutes of Health, grant number 5R21AR080388-02.

Institutional Review Board Statement: Not applicable.

Informed Consent Statement: Written informed consent has been obtained from the patient(s) to publish this paper.

Data Availability Statement: Not applicable.

Acknowledgments: The authors are in gratitude with the Soffer Family Foundation and the DRI Foundation for their generous funding support. The authors are in gratitude to CryoVida stem cell bank for their generous

donation of eMSC. These funding sources were not involved in any step of the study design, collection, analysis, or interpretation of the data, or writing of the manuscript.

Conflicts of Interest: The authors declare no conflict of interest.

References

1. Suvas, S., *Role of Substance P Neuropeptide in Inflammation, Wound Healing, and Tissue Homeostasis.* Journal of immunology (Baltimore, Md. : 1950), 2017. **199**(5): p. 1543-1552.
2. Okamura, Y., et al., *The dual regulation of substance P-mediated inflammation via human synovial mast cells in rheumatoid arthritis.* Allergol Int, 2017. **66s**: p. S9-s20.
3. Mashaghi, A., et al., *Neuropeptide substance P and the immune response.* Cellular and molecular life sciences : CMLS, 2016. **73**(22): p. 4249-4264.
4. Spitsin, S., et al., *Substance P–mediated chemokine production promotes monocyte migration.* Journal of Leukocyte Biology, 2017. **101**(4): p. 967-973.
5. Zieglgänsberger, W., *Substance P and pain chronicity.* Cell and tissue research, 2019. **375**(1): p. 227-241.
6. Lisowska, B., A. Lisowski, and K. Siewruk, *Substance P and Chronic Pain in Patients with Chronic Inflammation of Connective Tissue.* PloS one, 2015. **10**(10): p. e0139206-e0139206.
7. Koeck, F.X., et al., *Predominance of synovial sensory nerve fibers in arthrofibrosis following total knee arthroplasty compared to osteoarthritis of the knee.* Journal of Orthopaedic Surgery and Research, 2016. **11**(1): p. 25.
8. Lehner, B., et al., *Preponderance of sensory versus sympathetic nerve fibers and increased cellularity in the infrapatellar fat pad in anterior knee pain patients after primary arthroplasty.* Journal of Orthopaedic Research, 2008. **26**(3): p. 342-350.
9. Leyland, K.M., et al., *Knee osteoarthritis and time-to all-cause mortality in six community-based cohorts: an international meta-analysis of individual participant-level data.* Aging clinical and experimental research, 2021. **33**(3): p. 529-545.
10. Rizzo, M., et al., *Therapeutic Perspectives for Inflammation and Senescence in Osteoarthritis using Mesenchymal Stem Cells, Mesenchymal Stem Cell-Derived Extracellular Vesicles and Senolytic Agents* Cells, 2023(Ahead of Print).
11. Colombini, A., et al., *Mesenchymal stem cells in the treatment of articular cartilage degeneration: New biological insights for an old-timer cell.* Cytotherapy, 2019. **21**(12): p. 1179-1197.
12. Galipeau, J., et al., *International Society for Cellular Therapy perspective on immune functional assays for mesenchymal stromal cells as potency release criterion for advanced phase clinical trials.* Cytotherapy, 2016. **18**(2): p. 151-9.
13. Kotani, T., et al., *Anti-inflammatory and anti-fibrotic effects of intravenous adipose-derived stem cell transplantation in a mouse model of bleomycin-induced interstitial pneumonia.* Scientific Reports, 2018. **8**(1): p. 454.
14. Uccelli, A. and N.K. Rosbo, *The immunomodulatory function of mesenchymal stem cells: mode of action and pathways.* Annals of the New York Academy of Sciences, 2015. **1351**(1): p. 114-126.
15. Stagg, J. and J. Galipeau, *Mechanisms of Immune Modulation By Mesenchymal Stromal Cells and Clinical Translation.* Current molecular medicine, 2013. **13**.
16. Kouroupis, D., et al., *Single-Cell RNA-Sequencing Identifies Infrapatellar Fat Pad Macrophage Polarization in Acute Synovitis/Fat Pad Fibrosis and Cell Therapy.* Bioengineering (Basel), 2021. **8**(11).
17. Kouroupis, D., et al., *Infrapatellar fat pad-derived MSC response to inflammation and fibrosis induces an immunomodulatory phenotype involving CD10-mediated Substance P degradation.* Scientific Reports, 2019. **9**(1): p. 10864.
18. Sturiale, S., et al., *Neutral endopeptidase (EC 3.4.24.11) terminates colitis by degrading substance P.* Proceedings of the National Academy of Sciences of the United States of America, 1999. **96**(20): p. 11653-11658.
19. Kouroupis, D., L.D. Kaplan, and T.M. Best, *Human infrapatellar fat pad mesenchymal stem cells show immunomodulatory exosomal signatures.* Scientific Reports, 2022. **12**(1): p. 3609.
20. Nikfarjam, S., et al., *Mesenchymal stem cell derived-exosomes: a modern approach in translational medicine.* Journal of Translational Medicine, 2020. **18**(1): p. 449.
21. Leñero, C., et al., *CD146+ Endometrial-Derived Mesenchymal Stem/Stromal Cell Subpopulation Possesses Exosomal Secretomes with Strong Immunomodulatory miRNA Attributes.* Cells, 2022. **11**(24).
22. Pachler, K., et al., *A Good Manufacturing Practice–grade standard protocol for exclusively human mesenchymal stromal cell–derived extracellular vesicles.* Cytotherapy, 2017. **19**(4): p. 458-472.
23. Webber, J. and A. Clayton, *How pure are your vesicles?* Journal of extracellular vesicles, 2013. **2**: p. 10.3402/jev.v2i0.19861.
24. Chen, Y. and X. Wang, *miRDB: an online database for prediction of functional microRNA targets.* Nucleic Acids Research, 2019. **48**(D1): p. D127-D131.
25. Raudvere, U., et al., *g:Profiler: a web server for functional enrichment analysis and conversions of gene lists (2019 update).* Nucleic Acids Research, 2019. **47**(W1): p. W191-W198.

26. Kilkenny, C., et al., *Improving bioscience research reporting: the ARRIVE guidelines for reporting animal research.* PLoS biology, 2010. **8**(6): p. e1000412.
27. Udo, M., et al., *Monoiodoacetic acid induces arthritis and synovitis in rats in a dose- and time-dependent manner: proposed model-specific scoring systems.* Osteoarthritis and Cartilage, 2016. **24**(7): p. 1284-1291.
28. Ong, W.K., et al., *Identification of specific cell-surface markers of adipose-derived stem cells from subcutaneous and visceral fat depots.* Stem cell reports, 2014. **2**(2): p. 171-179.
29. Lv, F.-J., et al., *Concise Review: The Surface Markers and Identity of Human Mesenchymal Stem Cells.* Stem Cells, 2014. **32**(6): p. 1408-1419.
30. Maguer-Satta, V., R. Besançon, and E. Bachelard-Cascales, *Concise Review: Neutral Endopeptidase (CD10): A Multifaceted Environment Actor in Stem Cells, Physiological Mechanisms, and Cancer.* STEM CELLS, 2011. **29**(3): p. 389-396.
31. Xie, L., et al., *CD10-bearing fibroblasts may inhibit skin inflammation by down-modulating substance P.* Arch Dermatol Res, 2011. **303**(1): p. 49-55.
32. Bohnsack, M., et al., *Distribution of substance-P nerves inside the infrapatellar fat pad and the adjacent synovial tissue: a neurohistological approach to anterior knee pain syndrome.* Archives of Orthopaedic and Trauma Surgery, 2005. **125**(9): p. 592-597.
33. Kouroupis, D., et al., *CD10/neprilysin enrichment in infrapatellar fat pad-derived MSC under regulatory-compliant conditions: implications for efficient synovitis and fat pad fibrosis reversal.* The American Journal of Sports Medicine, 2020. **40**(8): p. 2013-2027.
34. Kouroupis, D., et al., *Regulatory-compliant conditions during cell product manufacturing enhance in vitro immunomodulatory properties of infrapatellar fat pad-derived mesenchymal stem/stromal cells.* Cytotherapy, 2020. **22**(11): p. 677-689.
35. Jung, E., et al., *The JNK-EGR1 signaling axis promotes TNF-α-induced endothelial differentiation of human mesenchymal stem cells via VEGFR2 expression.* Cell Death Differ, 2023. **30**(2): p. 356-368.
36. Gu, J., et al., *Identification and characterization of the novel Col10a1 regulatory mechanism during chondrocyte hypertrophic differentiation.* Cell Death & Disease, 2014. **5**(10): p. e1469-e1469.
37. Sasse, S., et al. *Angiogenic Potential of Bone Marrow Derived CD133+ and CD271+ Intramyocardial Stem Cell Trans- Plantation Post MI.* Cells, 2020. **9**, DOI: 10.3390/cells9010078.
38. Bakondi, B., et al., *CD133 Identifies a Human Bone Marrow Stem/Progenitor Cell Sub-population With a Repertoire of Secreted Factors That Protect Against Stroke.* Molecular Therapy, 2009. **17**(11): p. 1938-1947.
39. Battula, V.L., et al., *Isolation of functionally distinct mesenchymal stem cell subsets using antibodies against CD56, CD271, and mesenchymal stem cell antigen-1.* Haematologica-the Hematology Journal, 2009. **94**(2): p. 173-184.
40. Busser, H., et al., *Isolation and Characterization of Human Mesenchymal Stromal Cell Subpopulations: Comparison of Bone Marrow and Adipose Tissue.* Stem Cells and Development, 2015. **24**(18): p. 2142-2157.
41. Kohli, N., et al., *CD271-selected mesenchymal stem cells from adipose tissue enhance cartilage repair and are less angiogenic than plastic adherent mesenchymal stem cells.* Sci Rep, 2019. **9**(1): p. 3194.
42. Somoza, R.A., et al., *Chondrogenic Differentiation of Mesenchymal Stem Cells: Challenges and Unfulfilled Expectations.* Tissue Engineering. Part B, Reviews, 2014. **20**(6): p. 596-608.
43. Caron, M.M.J., et al., *Hypertrophic differentiation during chondrogenic differentiation of progenitor cells is stimulated by BMP-2 but suppressed by BMP-7.* Osteoarthritis and Cartilage, 2013. **21**(4): p. 604-613.
44. Mangiavini, L., et al., *Epidermal growth factor signalling pathway in endochondral ossification: an evidence-based narrative review.* Ann Med, 2022. **54**(1): p. 37-50.
45. Bowles, A.C., et al., *Signature quality attributes of CD146(+) mesenchymal stem/stromal cells correlate with high therapeutic and secretory potency.* Stem Cells, 2020. **38**(8): p. 1034-1049.
46. Zhang, X., M. Weng, and Z. Chen, *Fibroblast Growth Factor 9 (FGF9) negatively regulates the early stage of chondrogenic differentiation.* PLoS One, 2021. **16**(2): p. e0241281.
47. Terao, F., et al., *Fibroblast growth factor 10 regulates Meckel's cartilage formation during early mandibular morphogenesis in rats.* Developmental Biology, 2011. **350**(2): p. 337-347.
48. Caron, M.M.J., et al., *Aggrecan and COMP Improve Periosteal Chondrogenesis by Delaying Chondrocyte Hypertrophic Maturation.* Frontiers in Bioengineering and Biotechnology, 2020. **8**.
49. Wu, H., et al., *Engineered adipose-derived stem cells with IGF-1-modified mRNA ameliorates osteoarthritis development.* Stem Cell Research & Therapy, 2022. **13**(1): p. 19.
50. Curtale, G., et al., *An emerging player in the adaptive immune response: microRNA-146a is a modulator of IL-2 expression and activation-induced cell death in T lymphocytes.* Blood, 2010. **115**(2): p. 265-73.
51. Jurkin, J., et al., *miR-146a is differentially expressed by myeloid dendritic cell subsets and desensitizes cells to TLR2-dependent activation.* J Immunol, 2010. **184**(9): p. 4955-65.
52. Xu, D., et al., *Exosome-encapsulated miR-6089 regulates inflammatory response via targeting TLR4.* J Cell Physiol, 2019. **234**(2): p. 1502-1511.
53. Prieto-Potin, I., et al., *Characterization of multinucleated giant cells in synovium and subchondral bone in knee osteoarthritis and rheumatoid arthritis.* BMC Musculoskelet Disord, 2015. **16**: p. 226.

54. Greif, D.N., et al., *Infrapatellar Fat Pad/Synovium Complex in Early-Stage Knee Osteoarthritis: Potential New Target and Source of Therapeutic Mesenchymal Stem/Stromal Cells.* Frontiers in Bioengineering and Biotechnology, 2020. **8**(860).
55. Orecchioni, M., et al., *Macrophage Polarization: Different Gene Signatures in M1(LPS+) vs. Classically and M2(LPS–) vs. Alternatively Activated Macrophages.* Frontiers in Immunology, 2019. **10**.
56. Sierra-Filardi, E., et al., *CCL2 Shapes Macrophage Polarization by GM-CSF and M-CSF: Identification of CCL2/CCR2-Dependent Gene Expression Profile.* The Journal of Immunology, 2014. **192**(8): p. 3858.
57. De Luca, P., et al., *Human Diseased Articular Cartilage Contains a Mesenchymal Stem Cell-Like Population of Chondroprogenitors with Strong Immunomodulatory Responses.* J Clin Med, 2019. **8**(4).
58. Tu, J., et al., *Ontology and Function of Fibroblast-Like and Macrophage-Like Synoviocytes: How Do They Talk to Each Other and Can They Be Targeted for Rheumatoid Arthritis Therapy?* Frontiers in Immunology, 2018. **9**(1467).
59. Meng, Q. and B. Qiu, *Exosomal MicroRNA-320a Derived From Mesenchymal Stem Cells Regulates Rheumatoid Arthritis Fibroblast-Like Synoviocyte Activation by Suppressing CXCL9 Expression.* Front Physiol, 2020. **11**: p. 441.
60. Kulesza, A., L. Paczek, and A. Burdzinska, *The Role of COX-2 and PGE2 in the Regulation of Immunomodulation and Other Functions of Mesenchymal Stromal Cells.* Biomedicines, 2023. **11**(2): p. 445.
61. Lama, V., et al., *Prostaglandin E2 synthesis and suppression of fibroblast proliferation by alveolar epithelial cells is cyclooxygenase-2-dependent.* Am J Respir Cell Mol Biol, 2002. **27**(6): p. 752-8.
62. Jia, H., et al., *EGFR signaling is critical for maintaining the superficial layer of articular cartilage and preventing osteoarthritis initiation.* Proc Natl Acad Sci U S A, 2016. **113**(50): p. 14360-14365.
63. Lei, C.-T., et al., *MDM2 Contributes to High Glucose-Induced Glomerular Mesangial Cell Proliferation and Extracellular Matrix Accumulation via Notch1.* Scientific Reports, 2017. **7**(1): p. 10393.
64. Zhang, L., et al., *MDM2 promotes rheumatoid arthritis via activation of MAPK and NF-κB.* Int Immunopharmacol, 2016. **30**: p. 69-73.
65. Wen, C., et al., *Insulin-like growth factor-1 in articular cartilage repair for osteoarthritis treatment.* Arthritis Research & Therapy, 2021. **23**(1): p. 277.
66. Wiegand, N., et al., *Investigation of protein content of synovial fluids with DSC in different arthritides.* Journal of Thermal Analysis and Calorimetry, 2019. **138**(6): p. 4497-4503.
67. Macchi, V., et al., *The infrapatellar fat pad and the synovial membrane: an anatomo-functional unit.* Journal of Anatomy, 2018. **233**(2): p. 146-154.
68. Greif, D.N., et al., *Infrapatellar Fat Pad/Synovium Complex in Early-Stage Knee Osteoarthritis: Potential New Target and Source of Therapeutic Mesenchymal Stem/Stromal Cells.* Front Bioeng Biotechnol, 2020. **8**: p. 860.
69. Jones, E.A., et al., *Isolation and characterization of bone marrow multipotential mesenchymal progenitor cells.* Arthritis & Rheumatism, 2002. **46**(12): p. 3349-3360.
70. Johnstone, B., et al., *In vitro chondrogenesis of bone marrow-derived mesenchymal progenitor cells.* Exp Cell Res, 1998. **238**(1): p. 265-72.
71. Wang, W., D. Rigueur, and K.M. Lyons, *TGFβ signaling in cartilage development and maintenance.* Birth Defects Res C Embryo Today, 2014. **102**(1): p. 37-51.
72. van den Bosch, M.H., et al., *Canonical Wnt signaling skews TGF-β signaling in chondrocytes towards signaling via ALK1 and Smad 1/5/8.* Cell Signal, 2014. **26**(5): p. 951-8.
73. Li, L., et al., *Positive Effects of a Young Systemic Environment and High Growth Differentiation Factor 11 Levels on Chondrocyte Proliferation and Cartilage Matrix Synthesis in Old Mice.* Arthritis Rheumatol, 2020. **72**(7): p. 1123-1133.
74. Styczynska-Soczka, K., A.K. Amin, and A.C. Hall, *Cell-associated type I collagen in nondegenerate and degenerate human articular cartilage.* Journal of Cellular Physiology, 2021. **236**(11): p. 7672-7681.
75. Tsuchimochi, K., et al., *GADD45β Enhances Col10a1 Transcription via the MTK1/MKK3/6/p38 Axis and Activation of C/EBPβ-TAD4 in Terminally Differentiating Chondrocytes**. Journal of Biological Chemistry, 2010. **285**(11): p. 8395-8407.
76. Später, D., et al., *Wnt9a signaling is required for joint integrity and regulation of Ihh during chondrogenesis.* Development, 2006. **133**(15): p. 3039-49.
77. Malemud, C.J., *Inhibition of MMPs and ADAM/ADAMTS.* Biochem Pharmacol, 2019. **165**: p. 33-40.
78. Yang, C.Y., A. Chanalaris, and L. Troeberg, *ADAMTS and ADAM metalloproteinases in osteoarthritis - looking beyond the 'usual suspects'.* Osteoarthritis Cartilage, 2017. **25**(7): p. 1000-1009.
79. Rieppo, L., et al., *Histochemical quantification of collagen content in articular cartilage.* PLoS One, 2019. **14**(11): p. e0224839.
80. Nguyen, T.H., et al., *Mesenchymal Stem Cell-Derived Extracellular Vesicles for Osteoarthritis Treatment: Extracellular Matrix Protection, Chondrocyte and Osteocyte Physiology, Pain and Inflammation Management.* Cells, 2021. **10**(11).
81. Dowthwaite, G.P., et al., *The surface of articular cartilage contains a progenitor cell population.* J Cell Sci, 2004. **117**(6): p. 889-897.

 doi:10.20944/preprints202305.1465.v1

82. Kozhemyakina, E., et al., *Identification of a Prg4-expressing articular cartilage progenitor cell population in mice.* Arthritis Rheumatol, 2015. **67**(5): p. 1261-73.
83. Jiang, Y. and R.S. Tuan, *Origin and function of cartilage stem/progenitor cells in osteoarthritis.* Nat Rev Rheumatol, 2015. **11**(4): p. 206-12.
84. Koelling, S., et al., *Migratory Chondrogenic Progenitor Cells from Repair Tissue during the Later Stages of Human Osteoarthritis.* Cell Stem Cell, 2009. **4**(4): p. 324-335.